Inorganic Chemistry
Cite This: Inorg. Chem. XXXX, XXX, XXX–XXX
Article
pubs.acs.org/IC

A Bioactive L-Phenylalanine-Derived Arene in Multitargeted Organoruthenium Compounds: Impact on the Antiproliferative Activity and Mode of Action

Sanam Movassaghi,[†] Euphemia Leung,[‡] Muhammad Hanif,[†] Betty Y. T. Lee,[†] Hannah U. Holtkamp,[†] Jason K. Y. Tu,[†] Tilo Söhnel,[†] Stephen M. F. Jamieson,[‡] and Christian G. Hartinger*[,†]

[†]School of Chemical Sciences, University of Auckland, Private Bag 92019, Auckland 1142, New Zealand
[‡]Auckland Cancer Society Research Centre, University of Auckland, Private Bag 92019, Auckland 1142, New Zealand

Supporting Information

ABSTRACT: $Ru^{II}(\eta^6$-arene) compounds carrying bioactive flavonol ligands have shown promising anticancer activity against tumor cells via a multitargeting mode of action, i.e., through interaction with DNA and inhibition of topoisomerase IIα. By introducing a novel arene ligand based on the amino acid L-phenylalanine (Phe), we aimed to alter the pharmacological properties of the complexes. We report here a series of novel $Ru^{II}(\eta^6$-arene)Cl complexes with different substituents on the phenyl ring of the flavonol which should maintain the multitargeting capability of the parent η^6-*p*-cymene (cym) complexes. Studies with selected examples revealed stability in aqueous solution after quickly forming aqua complexes but rapid decomposition in pure DMSO. The reactions with protein and DNA models proceeded quickly and resulted in cleavage of the flavonol or adduct formation, respectively. The compounds were found to be cytotoxic with significant antiproliferative activity in cancer cells with IC_{50} values in the low μM range, while not following the same trends as observed for the cym analogues. Notably, the cellular accumulation of the new derivatives was significantly higher than for their respective cym complexes, and they induced DNA damage in a manner similar to that of cisplatin but to a lesser extent.

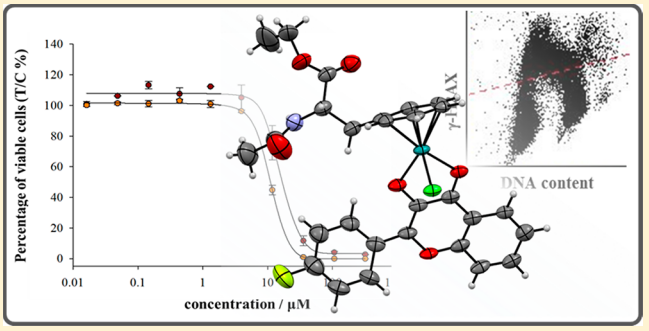

INTRODUCTION

Discovery of the anticancer activity of cisplatin has led to the development of metallopharmaceuticals based on a variety of metal centers.[1−3] Ruthenium complexes are considered the most promising next generation anticancer metallodrugs, and the Ru^{III} drug IT-139 (Chart 1, also known as NKP-1339), is undergoing clinical trials.[4−8] In the past decade, the field of organometallic anticancer agents has received considerable attention, and particularly $Ru^{II}(\eta^6$-arene) complexes have been widely investigated for their tunability and novel modes of action.[9−11] These properties are related to unique structural features of such half-sandwich "piano-stool" compounds which direct their specific interactions with target biomolecules.[12−19] The RAPTA family with the general formula [Ru(arene)(PTA)X_2] (PTA = 1,3,5-triaza-7-phosphatricyclo-[3.3.1.1]-decane; X = halido or dicarboxylato ligands) and the RAED compound class $[Ru(arene)Cl(en)]^+$ (en = 1,2-ethylenediamine) are the most advanced representatives of the Ru(arene) derivatives with their modes of action dependent on the ligands.[11,20]

Chart 1. Chemical Structures of Anticancer Ru Complexes

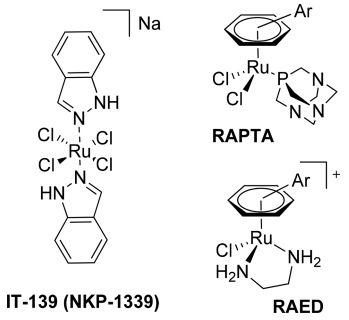

A recent approach in anticancer metallodrug design is to use nature-inspired, bioactive ligands such as 8-oxyquinoline,[21] quinolones,[22] curcumin derivatives,[23] chlorambucil,[17] non-steroidal anti-inflammatory drugs,[19,24] ethacrynic acid,[25,26] and flavonols[27] and coordinate them to biologically active metal centers. Flavonoids are secondary metabolites of plants with interesting biological properties such as antioxidant, anti-inflammatory, estrogenic, antimicrobial, and anticarcinogenic activity.[28,29] The 3-hydroxy-4-keto structural motif found in 3-hydroxyflavones coordinates bidentately to many metal ions and forms stable metal complexes with interesting applications

Received: May 2, 2018

DOI: 10.1021/acs.inorgchem.8b01187
Inorg. Chem. XXXX, XXX, XXX–XXX

and properties, such as intrinsic fluorescence.[30−33] One example for an application is the use as ligands in metal-based anticancer agents.[34−39] We reported a series of multitargeted anticancer Ru(arene) compounds carrying flavonol ligands with the metal center able to form covalent bonds to DNA, while the complex inhibits topoisomerase IIα.[27,33,40−42] The potent antiproliferative activity of the organoruthenium compounds was driven by the cytotoxicity of the flavonol ligands, and the complexes were more potent topoisomerase inhibitors than the flavonols which was also dependent on the substituents found at their phenyl ring.[27,40] However, the aqueous solubility of flavonols and their Ru(arene) complexes was limited. In the case of 8-oxyquinolinato complexes, we overcame this issue by replacing the apolar arene with an L-phenylalanine (Phe)-derived arene ligand.[43] Phe is bioactive and inhibits alkaline phosphatase, an enzyme which is overexpressed in many tumors.[44] Herein, we borrow the concept to study the impact of substituting η^6-*p*-cymene (cym) with the Phe-derived arene in 3-hydroxyflavonol Ru complexes on their biological activity and chemical properties in comparison to the analogous cym complexes.

EXPERIMENTAL SECTION

All reactions were performed in Schlenk flasks with dry solvents under nitrogen atmosphere. Chemicals acquired from commercial suppliers were used without any prior purification. Sodium methoxide was purchased from Fluka. Dry solvents were prepared according to standard methods.[45] [(η^6-Ethyl 2-acetamido-3-phenylpropanoate)-$Ru^{II}Cl_2]_2$[43] (**A**), **1a**^{cym},[27] and ligands **1**−**5**[33,40] were synthesized following literature procedures.

Elemental analyses were conducted on a vario EL cube (Elementar Analysensysteme GmbH, Hanau, Germany). 1D and 2D (^{1}H and ^{13}C HSQC and HMBC) NMR spectra were recorded on a Bruker Avance AVIII 400 MHz NMR spectrometer at ambient temperature at 400.13 MHz (^{1}H) or 100.57 MHz (^{13}C{^{1}H}). $CDCl_3$, D_2O, or DMSO-d_6 were used as NMR solvents. High resolution mass spectra were recorded on a Bruker micrOTOF-Q II ESI-MS in positive ion mode.

X-ray diffraction measurements of single crystals of **1a** were performed on a Rigaku Oxford Diffraction XtaLAB-Synergy-S single-crystal diffractometer with a PILATUS 200 K hybrid pixel array detector using Cu Kα radiation (λ = 1.54184 Å; Table S2). Single crystals of **1a**^{cym} were grown from a MeOH solution and analyzed on a Siemens/Bruker SMART APEX II Single Crystal Diffractometer with a CCD area detector using graphite monochromated Mo Kα radiation (λ = 0.71073 Å; Table S2). The data were processed with the SHELX2016 and Olex2 software packages.[46,47] All non-hydrogen atoms were refined anisotropically. Hydrogen atoms were inserted at calculated positions and refined with a riding model or without restrictions. Mercury 3.10 was used to visualize the molecular structure.

Biomolecule Interaction. The biomolecule interactions of **1a** were studied by ^{1}H NMR spectroscopy. It was dissolved in DMSO-d_6 and diluted with D_2O to obtain a 10% DMSO-d_6/D_2O solution. Equimolar amounts of the biomolecules L-methionine (Met), L-cysteine (Cys), L-histidine (His), or 9-ethylguanine (EtG) were added to **1a**, and NMR spectra were collected over periods of 48 h. In case of the reaction with EtG, **1a** was incubated with the DNA model at ratios of 1:1 and 2:1 (EtG:**1a**), and ^{1}H NMR spectra were recorded after 3 h of incubation.

Cellular Uptake. The cellular uptake experiments were carried out as described previously.[21,48] HCT116 cells were grown in αMEM (Life Technologies) supplemented with 5% fetal calf serum (Moregate Biotech) at 37 °C in a humidified incubator with 5% CO_2. HCT116 cells (4×10^5/well) were seeded into 6-well plates and allowed to settle for 24 h time at 37 °C and 5% CO_2. Compounds **1a** and **1a**^{cym} were dissolved in DMSO (379 and 443 μM, respectively) and diluted with media to a concentration of 1% DMSO to reach their previously determined IC_{50} values. The cells were incubated with metal complexes for 4 and 24 h, after which the medium was removed, and the cells were washed twice with 1 mL of ice-cold PBS buffer.

To determine the cell uptake of **1a** and **1a**^{cym} at the same concentration as the DNA-damaging ability was measured, stock solutions of 300 μM in DMSO were prepared and diluted with media to a concentration of 1% DMSO. The cells were incubated with the metal complexes for 6 h, after which the medium was removed, and the cells were washed twice with 1 mL of ice-cold PBS buffer.

The cells from all the experiments were lysed with 2 mL of concentrated nitric acid (containing 0.1 μL of a 1000 ± 3 μg/mL thulium as an internal standard) and digested with an Ethos Up microwave digestion system (Milestone). After the solutions were diluted with 10 mL of H_2O, the ruthenium content was determined by ICP-MS (Agilent 7700) with an ASX-500 autosampler (CETAC Technologies) in a Serie SuSi laminar flow hood (SPECTEC). The ICP-MS was equipped with a MicroMist nebulizer and a Scott double pass spray chamber. The carrier gas flow rate was 1 mL min^{-1}. The instrument was tuned for cerium, cobalt, lithium, magnesium, thallium, and yttrium. The reported values are the mean of at least three independent experiments conducted with blank wells for each substance to account for unspecific binding to the plastic of the well plates.

Cell Proliferation Assays. *Sulforhodamine B Cytotoxicity Assay.* HCT116, SW480, and NCI-H460 cells were supplied by ATCC, while SiHa cells were from Dr. David Cowan, Ontario Cancer Institute, Canada. The cells were grown in αMEM (Life Technologies) supplemented with 5% fetal calf serum (Moregate Biotech) at 37 °C in a humidified incubator with 5% CO_2.

The cells were seeded at 750 (HCT116, NCI-H460), 4000 (SiHa), or 5000 (SW480) cells/well in 96-well plates and left to settle for 24 h. The compounds were added to the plates in a series of 3-fold dilutions, containing a maximum of 0.5% DMSO at the highest concentration. The assay was terminated after 72 h by addition of 10% trichloroacetic acid (Merck Millipore) at 4 °C for 1 h. The cells were stained with 0.4% sulforhodamine B (Sigma-Aldrich) in 1% acetic acid for 30 min in the dark at room temperature and then washed with 1% acetic acid to remove unbound dye. The stain was dissolved in unbuffered Tris base (10 mM; Serva) for 30 min on a plate shaker in the dark and quantified on a BioTek EL808 microplate reader at an absorbance wavelength of 490 nm with 450 nm as the reference wavelength to determine the percentage of cell growth inhibition by determining the absorbance of each sample relative to a negative (no inhibitor) and a no-growth control (day 0). The IC_{50} values were calculated with SigmaPlot 12.5 using a three-parameter logistic sigmoidal dose−response curve between the calculated growth inhibition and the compound concentration. The presented IC_{50} values are the mean of at least three independent experiments, where 10 concentrations were tested in duplicate for each compound.

Thymidine Incorporation Assay. HCT116 cells were seeded at 750 per well in 96 well plates. The compounds were added to the plates in a series of 3-fold dilutions, containing a maximum of 0.5% DMSO at the highest concentration for 3 days. ^{3}H-Thymidine (0.04 μCi per well) was added to each well and incubated for 6 h. The cells were harvested on glass fiber filters using an automated TomTec harvester. The filters were incubated with Betaplate Scint and ^{3}H-thymidine incorporation was measured in a Trilux/Betaplate counter. The inhibition of ^{3}H-thymidine incorporation by the metal complexes was determined relative to the incorporation of ^{3}H-thymidine into DNA of control cells. The presented IC_{50} values are the means of two independent experiments, where 10 concentrations were tested in duplicate for each compound.

Flow Cytometry. HCT116 cells (7.2×10^5 cells per well) were plated in 6-well plates overnight and incubated with **1a**, **1a**^{cym}, cisplatin (30 μM each), doxorubicin (1 μM), and camptothecin (1 μM) for 6 h. Cells were harvested, fixed with 80% ethanol for 10 min, washed and resuspended in 1 mL of blocking buffer (1% FCS/PBS), and incubated with antibody to γH2AX (phosphorylated Ser139; Millipore, United States) in blocking buffer (1:500 dilution) at room

DOI: 10.1021/acs.inorgchem.8b01187
Inorg. Chem. XXXX, XXX, XXX−XXX

temperature for 2 h. Cells were washed, incubated with goat antimouse Alexa Fluor 488 Fab fragment secondary antibody (Invitrogen, New Zealand; 1:400 in blocking buffer for 1 h, at room temperature; dark), washed, and resuspended in 1 mL of blocking buffer containing RNase (1 μg/mL) and propidium iodide (PI; 10 μg/mL) for 10 min at room temperature. Antiphospho-Histone H2A.X (Ser139) Antibody, clone JBW301 (Millipore) and Alexa Fluor 488 (Life Technologies) were used according to the manufacturer instructions. Briefly, cells were harvested, fixed with 2% paraformaldehyde, permeabilized with 0.1% Triton-X, and incubated with antibody (5 μL in 300 μL blocking buffer for 2 h, at room temperature, dark), washed and resuspended in 1 mL of blocking buffer. Cells were analyzed in Becton Dickinson BD Accuri C6 flow cytometer.

General Procedure for the Synthesis of the Ru(η^6-ethyl-2-acetamido-3-phenylpropanoate) Complexes 1a−5a. A solution of [(η^6-*N*-acetyl-L-phenylalanine ethyl ester)$Ru^{II}Cl_2]_2$ **A** (0.45 equiv) in dry methanol (5 mL) was added to a solution of 3-hydroxyflavone **1**−**5** (1.00 equiv) and sodium methoxide (1.10 equiv) in a mixture of methanol (15 mL) and dichloromethane (5 mL). The reaction mixture was stirred at room temperature and under nitrogen atmosphere for 18 h. The solvent was evaporated in vacuo, and the residue was dissolved in dichloromethane and filtered. The complexes were precipitated from dichloromethane by addition of *n*-hexane.

*Chlorido[3-(oxo-κO)-2-(4-fluorophenyl)-chromen-4(1H)-onato-κO](η⁶-ethyl-2-acetamido-3-phenylpropanoate)ruthenium(II) (**1a**).* The reaction was performed according to the general procedure using **1** (100 mg, 0.39 mmol), NaOMe (23 mg, 0.43 mmol), and **A** (143 mg, 0.18 mmol) to afford **1a** as a deep red solid (193 mg, 72%). Single crystals suitable for X-ray diffraction analysis were grown from MeOH and CH_2Cl_2/diethyl ether. MS (ESI$^+$): *m*/*z* 592.0695 [M − Cl]$^+$ (m_{theor} = 592.0712). Elemental analysis calculated for $C_{28}H_{25}ClFNO_6Ru{\cdot}0.3CH_2Cl_2$: C 52.09, H 3.95, N 2.15%. Found: C 52.15, H 3.64, N 1.98%. ^{1}H NMR (400.13 MHz, $CDCl_3$): δ 1.20−1.37 (m, 6H, H11), 1.83 (s, 3H, $H13_{d1}$), 1.90 (s, 3H, $H13_{d2}$), 2.19−3.32 (m, 4H, H7), 4.21−4.34 (m, 4H, H10), 4.85−4.97 (m, 2H, H8), 5.41 (d, ^3J = 5 Hz, 2H, H_{arom}), 5.48 (t, ^3J = 6 Hz, 2H, H_{arom}), 5.38−5.51 (m, 4H, H_{arom}), 5.66−5.72 (m, 2H, H_{arom}), 5.77−5.88 (m, 4H, H_{arom}), 7.12−7.28 (m, 4H, H25/H27), 7.32−7.39 (m, 2H, H20), 7.54 (d, ^3J = 8 Hz, 2H, H21), 7.59−7.66 (m, 2H, H19), 7.77 (d, ^3J = 8 Hz, 2H, NH), 8.11−8.22 (m, 2H, H18), 8.47−8.58 (m, 4H, H24/H28) ppm. $^{13}C\{^1H\}$ NMR (100.57 MHz, $CDCl_3$): δ 14.3 (C11), 22.7 ($C13_{d1}$), 23.0 ($C13_{d2}$), 33.4 ($C7_{d1}$), 34.3 ($C7_{d2}$), 50.8 ($C8_{d1}$) 51.3 ($C8_{d2}$), 61.9 ($C10_{d1}$), 62.0 ($C10_{d2}$), 75.6 ($C4_{d2}$/$C4_{d2}$), 77.5 ($C6_{d1}$), 77.7 ($C6_{d2}$), 78.8 ($C3_{d1}$), 79.1 ($C3_{d2}$), 82.9 ($C2_{d1}$), 83.3 ($C2_{d2}$), 85.1 ($C5_{d1}$, $C5_{d2}$), 95.0 ($C1_{d1}$), 95.3 ($C1_{d2}$), 115.6 (d, $^2J_{C-F}$ = 21 Hz, $C25_{d1}$/$C27_{d1}$), 115.8 (d, $^2J_{C-F}$ = 21 Hz, $C25_{d2}$/$C27_{d2}$), 117.9 (C21), 119.9 (C22), 124.5 (C20), 124.6 (C18), 128.1 (C14), 129.6 (d, $^3J_{C-F}$ = 8 Hz, $C24_{d2}$/$C28_{d2}$), 129.7 (d, $^3J_{C-F}$ = 8 Hz, $C24_{d1}$/$C28_{d1}$), 132.1 ($C19_{d1}$), 132.2 ($C19_{d2}$), 146.7 (C23), 154.0 (C17), 155.1 (C15), 164.4 (C26), 170.6 ($C12_{d1}$), 171.2 ($C12_{d2}$), 171.5 (C9), 183.5 (C16) ppm.

*Chlorido[3-(oxo-κO)-2-(4-bromophenyl)-chromen-4-onato-κO]-(η⁶-ethyl-2-acetamido-3-phenylpropanoate)ruthenium(II) (**2a**).* The reaction was performed according to the general procedure using **2** (100 mg, 0.32 mmol), NaOMe (19 mg, 0.35 mmol), and **A** (116 mg, 0.14 mmol) to afford **2a** as a deep red solid (155 mg, 78%); MS (ESI$^+$): *m*/*z* 653.9889 [M − Cl]$^+$ (m_{theor} = 653.9901). Elemental analysis calculated for $C_{28}H_{25}ClBrNO_6Ru{\cdot}0.3CH_2Cl_2$: C 47.65, H 3.62, N 1.96%. Found: C 47.89, H 3.25, N 1.60%. ^{1}H NMR (400.13 MHz, $CDCl_3$): δ 1.22−1.37 (m, 6H, H11), 1.82 (s, 3H, $H13_{d1}$), 1.91 (s, 3H, $H13_{d2}$), 3.07−3.31 (m, 4H, H7), 4.21−4.33 (m, 4H, H10), 4.86−4.98 (m, 2H, H8), 5.42 (d, ^3J = 5 Hz, 2H, H_{arom}), 5.49 (t, ^3J = 6 Hz, 2H, H_{arom}), 5.65−5.73 (m, 2H, H_{arom}), 5.77−5.87 (m, 4H, H_{arom}), 7.32−7.39 (m, 2H, H20), 7.53 (d, ^3J = 8 Hz, 2H, H2), 7.57−7.72 (m, 8H, H25, H27, H19, NH), 8.13−8.22 (m, 2H, H18), 8.33−8.43 (m, 4H, H24/H28) ppm. $^{13}C\{^1H\}$ NMR (100.57 MHz, $CDCl_3$): δ 14.2 ($C11_{d1}$), 14.3 ($C11_{d1}$), 21.7 (C29), 22.6 ($C13_{d1}$), 22.9 ($C13_{d2}$), 33.2 ($C7_{d1}$), 33.9 ($C7_{d2}$), 50.8 ($C8_{d1}$) 51.2 ($C8_{d2}$), 61.8 ($C10_{d1}$), 61.9 ($C10_{d2}$), 75.8(C4), 77.6 ($C6_{d1}$), 77.7 ($C6_{d2}$), 78.8 ($C3_{d1}$), 79.1 ($C3_{d2}$), 83.0 ($C2_{d1}$), 83.3 ($C2_{d2}$), 85.4 (C5), 95.0 ($C1_{d1}$), 95.3 ($C1_{d2}$), 117.9 (C21), 119.9 (C22), 120.1 (C26), 124.4 (C20), 124.5 (C18), 128.7 (C24), 128.9 (C28), 130.8 (C14), 131.6 (C25), 131.9 (C27), 133.8 ($C19_{d1}$), 133.4 ($C19_{d2}$), 148.8 (C23), 153.6 (C17), 153.9 (C15), 171.2 (C12), 171.4 (C9), 183.7 (C16) ppm.

*Chlorido[3-(oxo-κO)-2-(4-methylphenyl)-chromen-4(1H)-onato-κO](η⁶-ethyl-2-acetamido-3-phenylpropanoate)ruthenium(II) (**3a**).* The reaction was performed according to the general procedure using **3** (100 mg, 0.40 mmol), NaOMe (20 mg, 0.44 mmol), and **A** (146 mg, 0.18 mmol) to afford **3a** as a deep red solid (170 mg, 68%). MS (ESI$^+$): *m*/*z* 588.0956 [M − Cl]$^+$ (m_{theor} = 588.0968). Elemental analysis calculated for $C_{29}H_{28}ClNO_6Ru{\cdot}0.1CH_2Cl_2$: C 55.34, H 4.50, N 2.22%. Found: C 55.30, H 4.12, N 1.82%. ^{1}H NMR (400.13 MHz, $CDCl_3$): δ 1.25−1.37 (m, 6H, H11), 1.75 (s, 3H, $H13_{d1}$), 1.89 (s, 3H, $H13_{d2}$), 2.39−2.46 (m, 6H, H29), 3.22−3.32 (m, 4H, H7), 4.22−4.34 (m, 4H, H10), 4.85−4.98 (m, 2H, H8), 5.37−5.42 (m, 2H, H_{arom}), 5.45−5.51 (m, 2H, H_{arom}), 5.66−5.73 (m, 2H, H_{arom}), 5.76−5.88 (m, 4H, H_{arom}), 7.27−7.38 (m, 6H, H25, H27, H20), 7.55 (d, ^3J = 8 Hz, 2H, H21), 7.58−7.64 (m, 2H, H19), 7.93 (d, ^3J = 8 Hz, 2H, NH), 8.13−8.21 (m, 2H, H18), 8.37 (d, ^3J = 8 Hz, 2H, $H24_{d1}$, $H28_{d1}$), 8.42 (d, ^3J = 8 Hz, 2H, $H24_{d2}$, $H28_{d2}$) ppm. $^{13}C\{^1H\}$ NMR (100.57 MHz, $CDCl_3$): δ 14.2 ($C11_{d1}$), 14.3 ($C11_{d1}$), 22.8 ($C13_{d1}$), 23.0 ($C13_{d2}$), 33.5 ($C7_{d1}$), 34.3 ($C7_{d2}$), 50.9 ($C8_{d1}$) 51.4 ($C8_{d2}$), 61.9 ($C10_{d1}$), 62.1 ($C10_{d2}$), 75.8 (C4), 77.6 ($C6_{d1}$), 77.8 ($C6_{d2}$), 78.9 ($C3_{d1}$), 79.2 ($C3_{d2}$), 82.9 ($C2_{d1}$), 83.3 ($C2_{d2}$), 84.9 (C5), 95.1 ($C1_{d1}$), 95.3 ($C1_{d2}$), 117.9 (C21), 120.1 (C22), 124.4 (C20), 124.5 (C18), 127. (C24) 127.6 (C28), 129.1(C14), 129.8 (C25), 129.4 (C27), 132.8 ($C19_{d1}$), 132.9 ($C19_{d2}$), 140.4 (C26), 150.7 (C23), 153.0 (C17), 154.0 (15), 170.8 (C12), 171.5 (C9), 183.1 (C16) ppm.

*Chlorido[3-(oxo-κO)-2-(4-trifluoromethylphenyl)-chromen-4-onato-κO](η⁶-ethyl-2-acetamido-3-phenylpropanoate)ruthenium-(II) (**4a**).* The reaction was performed according to the general procedure using **4** (100 mg, 0.33 mmol), NaOMe (19 mg, 0.36 mmol), and **A** (120 mg, 0.15 mmol) to afford **4a** as an orange solid (167 mg, 75%). MS (ESI$^+$): *m*/*z* 642.0692 [M − Cl]$^+$ (m_{theor} = 642.0680). Elemental analysis calculated for $C_{29}H_{25}ClF_3NO_6Ru{\cdot}2.5H_2O$: C 48.25, H 4.19, N 1.94%. Found: C 48.39, H 3.99, N 1.68%. ^{1}H NMR (400.13 MHz, $CDCl_3$): δ 1.27−1.36 (m, 6H, H11), 1.86 (s, 3H, $H13_{d1}$), 1.93 (s, 3H, $H13_{d2}$), 3.20−3.33 (m, 4H, H7), 4.22−4.33 (m, 4H, H10), 4.90−4.98 (m, 2H, H8), 5.45 (d, ^3J = 6 H, 2H, H_{arom}), 5.48−5.54 (m, 2H, H_{arom}), 5.71 (t, ^3J = 5 H, 2H, H_{arom}), 5.79−5.89 (m, 4H, H_{arom}), 7.35−7.41 (m, 2H, H20), 7.51 (d, ^3J = 8 Hz, 2H, NH), 7.58 (d, ^3J = 8 Hz, 2H, H2), 7.64−7.70 (m, 2H, H19), 7.72 (d, ^3J = 8 Hz, 4H, $H25_{d1}$, $H27_{d1}$), 7.77 (d, ^3J = 8 Hz, 4H, $H25_{d2}$, $H27_{d2}$), 8.16−8.24 (m, 2H, $H18_{d1+d2}$), 8.59−8.65 (m, 4H, H24, H28) ppm. $^{13}C\{^1H\}$ NMR (100.57 MHz, $CDCl_3$): δ 14.1 (C11), 22.8 ($C13_{d1}$), 23.0 ($C13_{d2}$), 33.8 ($C7_{d1}$), 34.5 ($C7_{d2}$), 50.9 ($C8_{d1}$) 51.4 ($C8_{d2}$), 62.0 ($C10_{d1}$), 62.1 ($C10_{d2}$), 76.1(C4), 77.6 ($C6_{d1}$), 77.7 ($C6_{d2}$), 77.9, 79.1 ($C3_{d1}$), 79.2 ($C3_{d2}$), 82.7 ($C2_{d1}$), 83.3 ($C2_{d2}$), 83.3, 84.6 ($C5_{d1}$, $C5_{d2}$), 95.3 ($C1_{d1}$), 95.5 ($C1_{d2}$), 118.0 (C21), 119.9 (C17), 124.6 (C21), 124.7 (C18), 125.4 (C29), 127.2 (C25), 127.4 (C27), 130.0 (C20), 130.8 (C23), 133.6 (C24), 133.7 (C19), 147.8 (C15), 154.2 (C14), 155.8 (C22), 165.5 (C12), 181.1 (C9), 184.7 (C16) ppm.

*Chlorido[3-(oxo-κO)-2-(3,4,5-trimethoxyphenyl)-chromen4-onato-κO](η⁶-ethyl-2-acetamido-3-phenylpropanoate)ruthenium-(II) (**5a**).* The reaction was performed according to the general procedure using **5** (100 mg, 0.30 mmol), NaOMe (18 mg, 0.33 mmol), and **A** (112 mg, 0.14 mmol) to afford **5a** as an orange solid (136 mg, 65%); MS (ESI$^+$): *m*/*z* 664.1131 [M − Cl]$^+$ (m_{theor} = 664.1124). Elemental analysis calculated for $C_{31}H_{32}ClNO_9Ru$: C 53.26, H 4.61, N 2.00%. Found: C 53.00, H 4.89, N 1.88%. ^{1}H NMR (400.13 MHz, $CDCl_3$): δ 1.26−1.35 (m, 6H, H11), 1.91 (s, 3H, $H13_{d1}$), 1.97 (s, 3H, $H13_{d2}$), 3.14−3.35 (m, 4H, H7), 3.93 (s, 3H, OMe), 3.99 (s, 6H, OMe), 4.19−4.30 (m, 4H, H10), 4.86−4.99 (m, 2H, H8), 5.42−5.53 (m, 4H, H_{arom}), 5.64−5.70 (m, 2H, H_{arom}), 5.72−5.87 (m, 4H, H_{arom}), 7.15−7.22 (m, 1H, $NH_)$, 7.33−7.41 (m, 2H, H20), 7.53−7.67 (m, 4H, H21, H19), 7.84 (s, 2H, $H24_{d1}$, $H28_{d1}$), 7.87 (s, 2H, $H24_{d2}$, $H28_{d2}$), 8.13−8.23 (m, 1H, H18) ppm. $^{13}C\{^1H\}$ NMR (100.57 MHz, $CDCl_3$): δ 14.1 (C11), 22.8 (C13),

DOI: 10.1021/acs.inorgchem.8b01187
Inorg. Chem. XXXX, XXX, XXX−XXX

Scheme 1. Preparation of Complexes 1a−5a

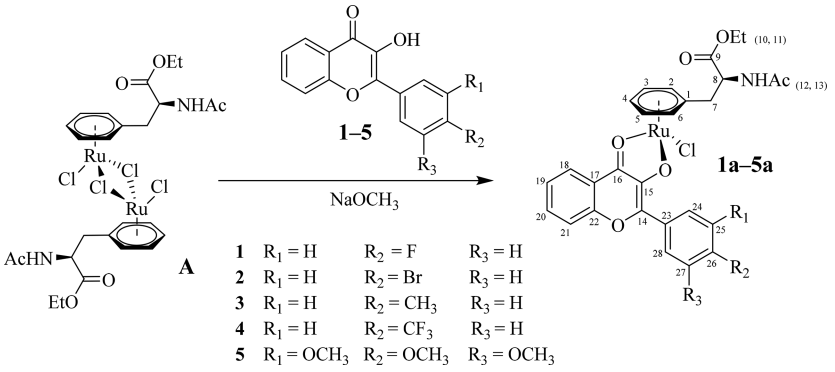

34.6 ($C7_{d1}$), 34.7 ($C7_{d2}$), 51.2 (C8), 56.3 (OMe), 61.0 (OMe), 62.0 (C10), 77.8 (C4), 78.7 (C6), 81.6 (C3), 82.9 (C2), 83.5 (C5), 94.9 (C1), 105.1 ($C24_{d1}$/$C28_{d1}$), 105.1 ($C24_{d2}$/$C28_{d2}$), 114.7 (C17), 117.7 (C21), 124.3 (C20), 124.4 ($C18_{d1}$), 124.5 ($C18_{d2}$), 132.7 (C23), 132.8 (C19), 138.7 (C14), 146.7 (C15), 153.0 (C25, C27), 161.8 (C22), 170.5 (C12), 171.1 (C9), 185.8 (C16) ppm.

RESULTS AND DISCUSSION

We recently reported a series of [Ru(arene)(8-oxyquinolinato)Cl] complexes in which we replaced the routinely used arene *p*-cymene with a protected Phe derivative. This modification maintained the in vitro anticancer activity of the complexes in the low μM range but improved the aqueous solubility significantly and may contribute to interaction of the complexes with other targets.[43] To expand this work on highly potent anticancer organometallics, we translate here this concept from *N*,*O*-chelating 8-oxyquinolinato complexes to *O*,*O*-donor systems as in 3-oxyflavonato ligands.[40,41] A series of substituted 3-hydroxyflavones **1**−**5** was used that had shown promising anticancer activity in the past upon coordination to metal centers, in particular **1**.[27,33,40−42] They were converted with the dimeric Ru precursor **A** into the respective organometallic compounds [Ru(η^6-*N*-acetyl-L-phenylalanine ethyl ester)(3-oxyflavonato)Cl] **1a**−**5a** (Scheme 1). The 3-hydroxyflavone derivatives were deprotonated using NaOMe, and **A** was added in dry MeOH. The reaction mixture was stirred at room temperature under nitrogen atmosphere for 18 h. The solvent was evaporated in vacuo, and the residue was dissolved in dichloromethane and filtered. Complexes **1a**−**5a** were obtained by precipitation with *n*-hexane in high yields of 65−78% (Scheme 1). The reaction results in the formation of diastereomers given the chiral nature of the Phe-derived arene ligand and another chiral center sitting at the Ru ion.

All synthesized compounds were characterized by standard methods including NMR spectroscopy, ESI-mass spectrometry, and elemental analysis. The ^{1}H NMR spectra show signals for the ethyl ester CH_3 in the range 1.22−1.37 ppm and around 1.90 ppm for the acetyl group. In both cases, we saw more than one set of signals owing to the diastereomeric nature of the complexes. Protons H7 and H8 of the Phe-derived arene ligand were found at ca. 3.3 and 4.2 ppm, respectively, while the 5 arene protons resonated in the range of 5.4−5.9 ppm. As expected, the signals assigned to the flavone ligand along with the amide NH were found between 7.1 and 8.7 ppm. These signals are in similar ranges as observed for structurally related 8-oxyquinolinato complexes.[43] The ESI-MS results confirmed the nature of compounds with $[M - Cl]^+$ ions detected for complexes **1a**−**5a** in positive ion mode.

Single crystals of **1a** were grown by slow diffusion of diethyl ether into a mixture of methanol/dichloromethane (approximately 1:1) and analyzed by X-ray diffraction analysis (Figure 1). A diastereomer of the complex crystallized in the

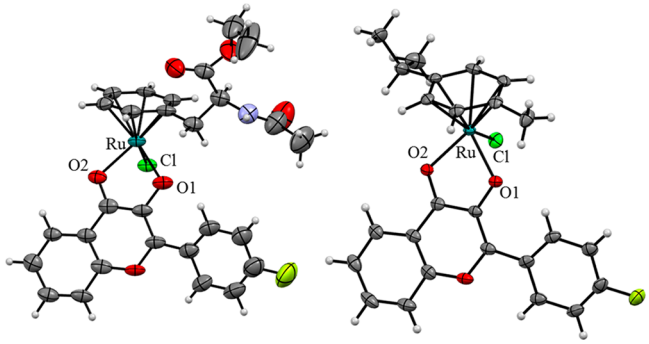

Figure 1. Molecular structures of a crystallized diastereomer of **1a** and of an enantiomer of $\mathbf{1a}^{cym}$ drawn at 50% probability level. Cocrystallized solvent molecules were omitted for clarity.

monoclinic space group $P2_1$. The compound features the pseudo-octahedral piano-stool configuration around the metal center[10,22] and is involved in a network of hydrogen bonds through cocrystallized water molecules. The amide carbonyl oxygen atom forms a hydrogen bond with a water molecule, which bridges it to another molecule of **1a** through an interaction with the amide NH proton. Another H bond was found for **1a** from the deprotonated flavone O atom to another water molecule. The flavone backbone is involved in intermolecular π-stacking interactions, and the shortest distance is 3.425 Å (Figure S1). The Ru−$arene_{centroid}$ distance is found at 1.638 Å (Table 1). The 3-oxyflavonato ligand forms a virtually planar five-membered metallocycle with the Ru center, while the phenyl substituent of the ligands are twisted with torsion angles of 29.1°. The two Ru−O bond lengths are very similar at 2.068(5) and 2.117(6) Å, with the longer bonds formed between the Ru and flavone-carbonyl O atoms. The C15−O1 bond is significantly longer (1.374(8) Å) than the C16−O2 distance (1.259(8) Å), indicating higher single bond character. The Ru−Cl bond length is 2.423(2) Å. Comparison of these structural parameters with those of the analogous *p*-cymene complex $\mathbf{1a}^{cym}$ (crystals of a mixture of enantiomers were grown from MeOH; Figure 1) shows that the Ru−Cl bond is slightly longer than in $\mathbf{1a}^{cym}$ (2.4326(10) Å). The Ru−O1 distance is slightly shorter, while the other distances

DOI: 10.1021/acs.inorgchem.8b01187
Inorg. Chem. XXXX, XXX, XXX−XXX

Table 1. Key Bond Lengths (Å) and Angles (°) for Complex 1a in Comparison to the Analogous *p*-Cymene Complex $1a^{cym}$

	1a	$1a^{cym}$
bond lengths (Å) Ru–arene$_{centroid}$		
	1.638	1.639
Ru–Cl	2.423(2)	2.4186(6)
Ru–O1	2.068(4)	2.078(2)
Ru–O2	2.117(6)	2.112(2)
torsion angles (deg)		
C15–C14–C23–C24	29(1)	14.1(4)
bond angles (deg)		
C1–Ru–O1	84.8(2)	85.41(5)
C1–Ru–O2	83.98(13)	86.00(5)
O1–Ru–O2	79.4(2)	78.39(7)

around the Ru center are similar (Table 1).[27,40] The most notable difference is the more planar nature of the 3-oxyflavonato ligand in $1a^{cym}$ as compared to **1a**.

Stability in DMSO and Aqueous Solution. The stability in DMSO and water was determined for **1a** as a representative example for the compound class with ^{1}H NMR spectroscopy over a time span of two days. The complex was stable in DMSO-d_6 for less than 1 h, after which additional sets of signals appeared in the ^{1}H NMR spectra, probably due to a combination of cleavage of the arene ligand and additional ligand exchange reactions at the metal center (Figure S2). When stability studies were carried out at low concentrations of DMSO-d_6 (10% in D_2O), an immediate chlorido/aqua ligand exchange was observed (Figure 2). This was confirmed

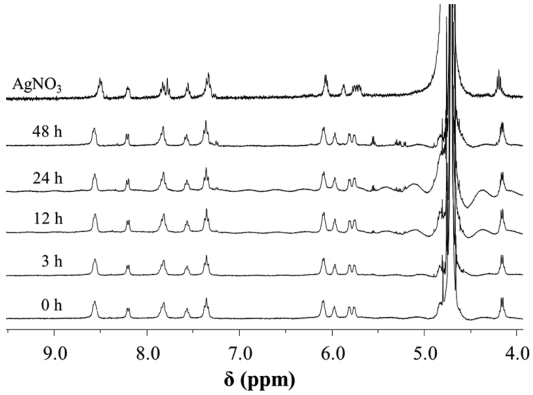

Figure 2. ^{1}H NMR spectroscopy study on the stability of **1a** in 10% DMSO-d_6 in D_2O over a period of 48 h.

by the addition of 1 equiv of $AgNO_3$, which resulted in the same spectrum as recorded over the 48 h period. These experiments demonstrate that the compounds are sufficiently stable to carry out cell viability studies under conditions routinely used in biological assays.

Biomolecule Interaction. Metal complexes are prone to undergo ligand exchange reactions, especially in biological systems with many binding partners available. These interactions may be beneficial and support the accumulation of the pharmacophore in the desired tissue or allow interaction with the target. On the other hand, these reactions may deactivate drugs. To understand the nature of interactions of the novel organoruthenium compounds with biomolecules such as proteins and DNA, we reacted **1a** with the biomolecules L-cysteine (Cys), L-methionine (Met), L-histidine, and 9-ethylguanine (EtG) in 10% DMSO-d_6/D_2O, and the progress of the reactions was monitored by ^{1}H NMR spectroscopy. The spectra recorded for the reaction mixtures with the amino acids revealed that the signals assigned to the flavone protons vanished very rapidly (Figures 3 and S3), while

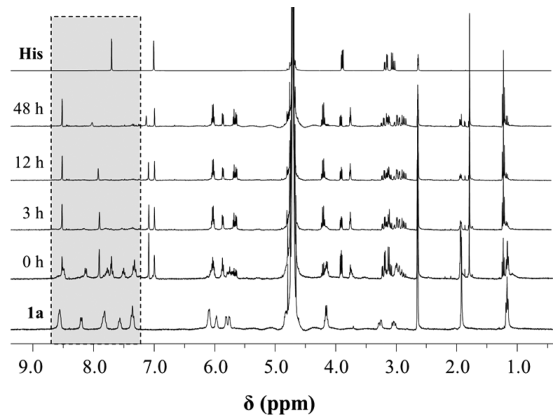

Figure 3. ^{1}H NMR spectroscopy study on the reaction of **1a** with His (1:1) in 10% DMSO-d_6/D_2O over a period of 48 h.

in the region of the spectra characteristic for the arene ligand, additional signals formed. These are most likely from the formed amino acid complexes upon coordination to the Ru center. During the experiments, in particular with Cys, precipitation was observed, which is not unsurprising given the low aqueous solubility of 3-hydroxyflavones when cleaved from the metal center.

DNA has been suggested as the target for the RAED anticancer agents.[49] The reaction of **1a** with the DNA model EtG resulted in the formation of EtG complexes after ligand exchange with Cl^-. The reaction between **1a** and EtG in a molar ratio of 1:1 proceeded very quickly, and already 1 h after the start of the incubation, the complex was transformed quantitatively into its EtG adduct (Figure S4). This is supported by an experiment in which a second equivalent of EtG was added to the reaction mixture, and the peak assigned to unreacted EtG at 7.88 ppm grew while the rest of the spectrum remained unchanged (Figure 4). Both reaction mixtures were also analyzed by ESI-MS in positive ion mode. For example, the mass spectrum recorded from the 1:1 reaction mixture showed a peak at m/z 773.1609, which was

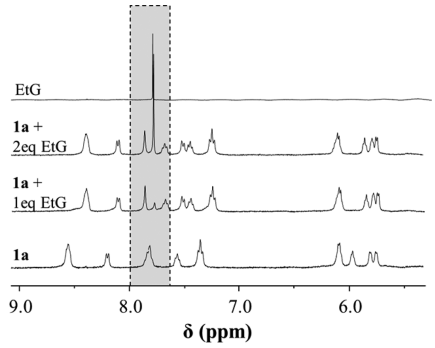

Figure 4. ^{1}H NMR spectroscopy study on the reaction of **1a** with 1 or 2 equiv of EtG in 10% DMSO-d_6/D_2O after an incubation period of 3 h.

DOI: 10.1021/acs.inorgchem.8b01187
Inorg. Chem. XXXX, XXX, XXX–XXX

assigned to the ion $[\mathbf{1a} + EtG - Cl]^+$ (m_{theor} = 773.1661), while the base peak was identified as $[\mathbf{1a} - Cl]^+$ (Figure S5). The low abundance of the adduct peak relative to the latter species may be explained by the low stability of the EtG adduct in the gas phase. As the samples were prepared in deuterated solvents, species were detected in which protons had exchanged with deuterium.

In Vitro Cytotoxicity against Human Cancer Cells and Cellular Accumulation. The in vitro antiproliferative activity of complexes **1a**–**5a** was studied in HCT116 human colorectal, NCI-H460 non-small cell lung, SiHa cervical carcinoma, and SW480 colon adenocarcinoma cells using the sulforhodamine B assay (SRB; Table 2) and compared to the

Table 2. In Vitro Cytotoxic Activity of Compounds 1a–5a in the Human Cancer Cell Lines HCT116 (Colon), NCI-H460 (Nonsmall Cell Lung), SiHa (Cervix), and SW480 (Colon)[a]

	IC_{50} values (μM)			
compound	HCT116	NCI-H460	SiHa	SW480
1a	4.4 ± 0.4	2.4 ± 0.1	22 ± 1	9.5 ± 0.4
2a	2.1 ± 0.1	1.5 ± 0.1	15 ± 1	5.7 ± 0.1
3a	2.8 ± 0.2	2.0 ± 0.2	19 ± 2	7.2 ± 0.3
4a	1.3 ± 0.1	1.0 ± 0.3	13 ± 2	2.5 ± 0.1
5a	8.3 ± 1.9	5.9 ± 0.8	20 ± 1	8.1 ± 0.1
1a^{cym}	3.8 ± 0.1	2.7 ± 0.5	23 ± 1	7.2 ± 0.4
2a^{cym}	3.4 ± 0.2	2.9 ± 0.6	29 ± 1	8.5 ± 0.7
3a^{cym}	5.8 ± 0.8	5.4 ± 0.3	22 ± 4	13 ± 4
4a^{cym}	8.7 ± 0.1	9.2 ± 1.1	64 ± 6	21 ± 0.3
5a^{cym}	14 ± 1	14 ± 1	41 ± 2	30 ± 1

[a]The IC_{50} values are given as means ± standard deviation.

cytotoxic activity of the analogous cym complexes **1a^{cym}**–**5a^{cym}**. All Ru^{II}(arene)–flavonoid complexes were potent antiproliferative agents with IC_{50} values in the low micromolar range, especially in HCT116 and NCI-H460 cells. Compound **4a** with its trifluoromethyl substituent was the most potent derivative, while the trismethoxy (**5a**) and the fluoro (**1a**) derivatives were the least active, depending on the cell line used. This trend is in contrast to that found for the analogous cym complexes **1a^{cym}**–**5a^{cym}**, for which the CF_3 (**4a^{cym}**) derivative was among the least active compounds, while the *p*-fluoro (**1a^{cym}**) complex was the most potent compounds. The introduction of the protected Phe group as an arene had a significant impact on the cytotoxicity of complexes with ligands **2**–**5**, which all became more cytotoxic, while **1a** was similarly potent to its cym analogue **1a^{cym}**. We found a similar effect for hydroxyquinoline complexes, where the introduction of the Phe-based arene ligand also resulted in complexes with limited correlation of their cytotoxic activity to those of the parent cym complexes.[43] These results suggest that organoruthenium compounds with the Phe-derived arene may have different modes of action and that the biological activity is not necessarily a function of the lipophilicity and associated increased cell penetration ability. This conclusion is also supported by cellular accumulation data for **1a** and **1a^{cym}**. The cellular Ru content after treatment of HCT116 cells with these complexes at concentrations similar to their IC_{50} values (3.79 μM for **1a^{cym}** and 4.43 μM for **1a**) was measured after 4 and 24 h by inductively coupled plasma mass spectrometry. After incubation of the cells with the compounds for 4 h, only **1a** was found to enter the cells, while the detected amount of **1a^{cym}** was negligible. Increasing the incubation time to 24 h resulted in significantly higher Ru levels for both compounds (Figure 5); however, overall the Ru content for **1a** was about 5

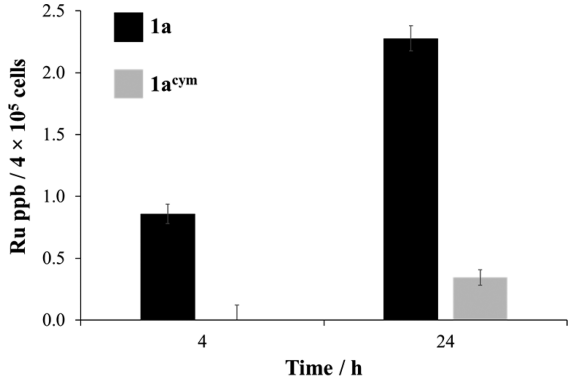

Figure 5. Cellular accumulation of **1a** and **1a^{cym}** determined by ICP-MS after treatment of HCT116 cells for 4 and 24 h.

times higher than that found for **1a^{cym}**, despite similar in vitro cytotoxicity which was, however, determined over 72 h. Note that **1a^{cym}** was strongly interacting with the well plates, resulting in significant blanks which were considered when determining the cellular accumulation.

In addition, the in vitro antiproliferative activity of complexes **1a** and **1a^{cym}** in HCT116 cells was compared to that of cisplatin in SRB and ^{3}H-thymidine incorporation (TI) assays (Figures 6 and S6, Table S2). Overall, the two assays

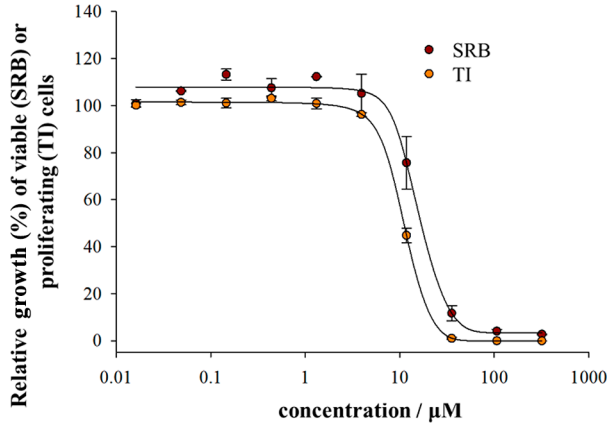

Figure 6. Relative growth (%) of HCT116 cells measured by the SRB and TI assays, respectively, after incubation with **1a** for 72 h.

gave similar IC_{50} values for all compounds, although the values were slightly higher by SRB assay, especially for cisplatin. This supports that the organometallics are cytotoxic rather than cytostatic.

Induction of DNA Damage by 1a and 1a^{cym}. As pointed out earlier, metal complexes are prone to undergo ligand exchange reactions with biomolecules, and the flavone complexes were designed to act as enzyme inhibitors while still being able to coordinate to DNA. Therefore, we examined whether the antiproliferative effect of **1a** and **1a^{cym}** is related to DNA damage. For this purpose, HCT116 cells were exposed to **1a**, **1a^{cym}**, cisplatin (30 μM each), doxorubicin (1 μM), and camptothecin (1 μM). The DNA damage response was measured by the level of γH2AX phosphorylation using flow

DOI: 10.1021/acs.inorgchem.8b01187
Inorg. Chem. XXXX, XXX, XXX–XXX

cytometry as compared to control (Figure 7). Camptothecin specifically induces DNA damage in the S phase, while the

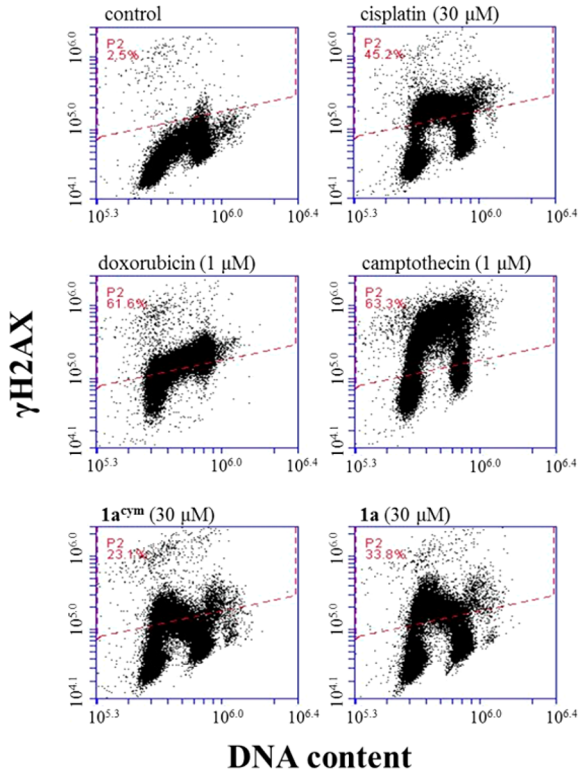

Figure 7. DNA damaging ability in HCT116 cells as determined for γH2AX by flow cytometry after treatment with **1a**, **1a**^{cym}, cisplatin (30 μM each), doxorubicin (1 μM), and camptothecin (1 μM) for 6 h.

DNA damage caused by doxorubicin is cell phase independent. Both **1a** and **1a**^{cym} showed very similar DNA damaging ability, which is surprising given the differing cellular accumulation. The amount of Ru in the cells at 6 h was found to be about 4 times higher for **1a** over **1a**^{cym} when they were treated with the compounds at the same concentration as used for the flow cytometry sample preparation (30 μM; data not shown). The DNA damage profile of **1a** and **1a**^{cym} after 6 h treatment is unlike that of both camptothecin and doxorubicin but resembles to some extent that of cisplatin (Figure 7). Cisplatin was reported to induce an S/G2 cell cycle arrest and apoptosis in V79 cells,[50] which supports a similar conclusion for the compounds studied here. However, the induction level of γH2AX phosphorylation was significantly lower with averages of 27% for **1a** and 24% for **1a**^{cym} as compared to 45% for cisplatin. This may be a result of the higher lability of the DNA−metal bonds for Ru^{II} as compared to those for Pt^{II}. Also, cisplatin forms bifunctional adducts, whereas DNA can coordinate to the organoruthenium compounds only monodentately.

Exposure of cells to **1a** and **1a**^{cym} for 24 h at concentrations of 30 and 60 μM revealed that both compounds induced higher dose-dependent DNA damage than the damage response found after 6 h, as was indicated by a higher number of cells expressing γH2AX (Figure S7). In all cases, **1a** caused slightly more DNA damage than its cym counterpart, which may explain the slightly differing antiproliferative activity of the compounds. This was especially pronounced in the samples containing only 30 μM of the compounds.

CONCLUSIONS

The design concept of coordinating bioactive ligands to metal centers resulted in the preparation of [Ru(η^6-*p*-cymene)-(flavonolato)Cl] compounds with interesting biological activity defined by its flavonolato ligand and the properties of the metal center. We have borrowed here a concept in which we replace the commonly used arene cym with a recently introduced novel arene derived from the bioactive amino acid L-phenylalanine, which may add to the biological activity of the complex. The synthesis and characterization of the series of organoruthenium compounds was complemented with studies on the stability in water and DMSO, as well as the reactivity with biomolecules. High stability in aqueous solution after dissolution in DMSO was demonstrated for a representative example of the complexes, after rapidly forming aqua complexes. In contrast, the complex quickly decomposed in DMSO, as determined by NMR spectroscopy. The reactions with the amino acids His, Met, and Cys showed quick cleavage of the flavonolato ligand from the Ru center, while incubation with EtG resulted in substitution of the chlorido ligand with the DNA model compound. All new compounds were potent anticancer agents in a panel of cancer cells with IC_{50} values as low as 1 μM in NCI-H460 non-small cell lung cancer cells. The IC_{50} values of the Phe-derived compounds did not follow the same trends as observed for their cym analogues, but the values were in a similar range. This is surprising given that the cellular accumulation of a representative Phe-derived complex was found to be much higher than of its cym analogue, independent of the concentration used and the incubation times. Comparison of the IC_{50} values determined by ^{3}H-thymidine incorporation and sulforhodamine B assays revealed cytotoxic rather than cytostatic activity. As the compounds were designed to be able to coordinate to DNA, which was confirmed in the reactivity studies with EtG, it is important to note that they damage DNA, which may contribute to their cytotoxic activity. The DNA damage profile was similar to that of cisplatin; however, the amount of DNA damage detected was lower for the tested compounds than for cisplatin. These data support the hypothesized DNA binding ability of the compounds while not contradicting the topoisomerase inhibitory activity, which was demonstrated for the parent compounds, as another contributor to the biological activity.

ASSOCIATED CONTENT

Supporting Information

The Supporting Information is available free of charge on the ACS Publications website at DOI: 10.1021/acs.inorgchem.8b01187.

X-ray crystallographic data and measurement parameters, NMR and mass spectrometric analysis of stability and reactivity with biomolecules, and additional data collected in in vitro anticancer activity and mode of action studies (PDF)

Accession Codes

CCDC 1840317 and 1840404 contain the supplementary crystallographic data for this paper. These data can be obtained free of charge via www.ccdc.cam.ac.uk/data_request/cif, by emailing data_request@ccdc.cam.ac.uk, or by contacting The Cambridge Crystallographic Data Centre, 12 Union Road, Cambridge CB2 1EZ, UK; fax: +44 1223 336033.

DOI: 10.1021/acs.inorgchem.8b01187
Inorg. Chem. XXXX, XXX, XXX−XXX

AUTHOR INFORMATION

Corresponding Author

*E-mail: c.hartinger@auckland.ac.nz; Tel.: +64 9 3737 599 ext. 83220; Website: http://www.hartinger.auckland.ac.nz.

ORCID

Muhammad Hanif: 0000-0002-2256-2317

Christian G. Hartinger: 0000-0001-9806-0893

Notes

The authors declare no competing financial interest.

ACKNOWLEDGMENTS

We thank the University of Auckland (University of Auckland Doctoral Scholarships to H.H. and B.L.) for the financial support. We are grateful to Tanya Groutso for collecting the single crystal X-ray diffraction data, to Tony Chen for ESI-MS analyses, and to Marjan Askarian-Amiri for useful discussions.

REFERENCES

(1) Kelland, L. The resurgence of platinum-based cancer chemotherapy. *Nat. Rev. Cancer* **2007**, *7*, 573−584.

(2) Jakupec, M. A.; Galanski, M.; Arion, V. B.; Hartinger, C. G.; Keppler, B. K. Antitumour metal compounds: more than theme and variations. *Dalton Trans.* **2008**, 183−194.

(3) Hanif, M.; Hartinger, C. G. Anticancer metallodrugs: where is the next cisplatin? *Future Med. Chem.* **2018**, *10*, 615−617.

(4) Hartinger, C. G.; Jakupec, M. A.; Zorbas-Seifried, S.; Groessl, M.; Egger, A.; Berger, W.; Zorbas, H.; Dyson, P. J.; Keppler, B. K. KP1019, A New Redox-Active Anticancer Agent - Preclinical Development and Results of a Clinical Phase I Study in Tumor Patients. *Chem. Biodiversity* **2008**, *5*, 2140−2155.

(5) Trondl, R.; Heffeter, P.; Kowol, C. R.; Jakupec, M. A.; Berger, W.; Keppler, B. K. NKP-1339, the first ruthenium-based anticancer drug on the edge to clinical application. *Chem. Sci.* **2014**, *5*, 2925−2932.

(6) Alessio, E. Thirty Years of the Drug Candidate NAMI-A and the Myths in the Field of Ruthenium Anticancer Compounds: A Personal Perspective. *Eur. J. Inorg. Chem.* **2017**, *2017*, 1549−1560.

(7) Zeng, L.; Gupta, P.; Chen, Y.; Wang, E.; Ji, L.; Chao, H.; Chen, Z.-S. The development of anticancer ruthenium(II) complexes: from single molecule compounds to nanomaterials. *Chem. Soc. Rev.* **2017**, *46*, 5771−5804.

(8) Notaro, A.; Gasser, G. Monomeric and dimeric coordinatively saturated and substitutionally inert Ru(II) polypyridyl complexes as anticancer drug candidates. *Chem. Soc. Rev.* **2017**, *46*, 7317.

(9) Noffke, A. L.; Habtemariam, A.; Pizarro, A. M.; Sadler, P. J. Designing organometallic compounds for catalysis and therapy. *Chem. Commun.* **2012**, *48*, 5219−5246.

(10) Hartinger, C. G.; Metzler-Nolte, N.; Dyson, P. J. Challenges and Opportunities in the Development of Organometallic Anticancer Drugs. *Organometallics* **2012**, *31*, 5677−5685.

(11) Murray, B. S.; Babak, M. V.; Hartinger, C. G.; Dyson, P. J. The development of RAPTA compounds for the treatment of tumors. *Coord. Chem. Rev.* **2016**, *306*, 86−114.

(12) Habtemariam, A.; Melchart, M.; Fernandez, R.; Parsons, S.; Oswald, I. D. H.; Parkin, A.; Fabbiani, F. P. A.; Davidson, J. E.; Dawson, A.; Aird, R. E.; Jodrell, D. I.; Sadler, P. J. Structure-Activity Relationships for Cytotoxic Ruthenium(II) Arene Complexes Containing N,N-, N,O-, and O,O-Chelating Ligands. *J. Med. Chem.* **2006**, *49*, 6858−6868.

(13) Tan, Y. Q.; Dyson, P. J.; Ang, W. H. Acetal-functionalized RAPTA complexes for conjugation and labeling. *Organometallics* **2011**, *30*, 5965−5971.

(14) Nowak-Sliwinska, P.; van Beijnum, J. R.; Casini, A.; Nazarov, A. A.; Wagnieres, G.; van den Bergh, H.; Dyson, P. J.; Griffioen, A. W. Organometallic Ruthenium(II) Arene Compounds with Antiangiogenic Activity. *J. Med. Chem.* **2011**, *54*, 3895−3902.

(15) Kilpin, K. J.; Clavel, C. M.; Edafe, F.; Dyson, P. J. Naphthalimide-Tagged Ruthenium-Arene Anticancer Complexes: Combining Coordination with Intercalation. *Organometallics* **2012**, *31*, 7031−7039.

(16) Hanif, M.; Nazarov, A. A.; Legin, A.; Groessl, M.; Arion, V. B.; Jakupec, M. A.; Tsybin, Y. O.; Dyson, P. J.; Keppler, B. K.; Hartinger, C. G. Maleimide-functionalised organoruthenium anticancer agents and their binding to thiol-containing biomolecules. *Chem. Commun.* **2012**, *48*, 1475−1477.

(17) Nazarov, A. A.; Meier, S. M.; Zava, O.; Nosova, Y. N.; Milaeva, E. R.; Hartinger, C. G.; Dyson, P. J. Protein ruthenation and DNA alkylation: chlorambucil-functionalized RAPTA complexes and their anticancer activity. *Dalton Trans.* **2015**, *44*, 3614−3623.

(18) Babak, M. V.; Meier, S. M.; Huber, K. V. M; Reynisson, J.; Legin, A. A.; Jakupec, M. A.; Roller, A.; Stukalov, A.; Gridling, M.; Bennett, K. L.; Colinge, J.; Berger, W.; Dyson, P. J.; Superti-Furga, G.; Keppler, B. K.; Hartinger, C. G. Target profiling of an antimetastatic RAPTA agent by chemical proteomics: relevance to the mode of action. *Chem. Sci.* **2015**, *6*, 2449−2456.

(19) Păunescu, E.; McArthur, S.; Soudani, M.; Scopelliti, R.; Dyson, P. J. Nonsteroidal Anti-inflammatory—Organometallic Anticancer Compounds. *Inorg. Chem.* **2016**, *55*, 1788−1808.

(20) Adhireksan, Z.; Davey, G. E.; Campomanes, P.; Groessl, M.; Clavel, C. M.; Yu, H. J.; Nazarov, A. A.; Yeo, C. H. F.; Ang, W. H.; Droge, P.; Rothlisberger, U.; Dyson, P. J.; Davey, C. A. Ligand substitutions between ruthenium-cymene compounds can control protein versus DNA targeting and anticancer activity. *Nat. Commun.* **2014**, *5*, 1.

(21) Kubanik, M.; Holtkamp, H.; Söhnel, T.; Jamieson, S. M. F.; Hartinger, C. G. Impact of the Halogen Substitution Pattern on the Biological Activity of Organoruthenium 8-Hydroxyquinoline Anticancer Agents. *Organometallics* **2015**, *34*, 5658−5668.

(22) Kljun, J.; Bytzek, A. K.; Kandioller, W.; Bartel, C.; Jakupec, M. A.; Hartinger, C. G.; Keppler, B. K.; Turel, I. Physicochemical Studies and Anticancer Potency of Ruthenium η^6-p-Cymene Complexes Containing Antibacterial Quinolones. *Organometallics* **2011**, *30*, 2506−2512.

(23) Pettinari, R.; Marchetti, F.; Condello, F.; Pettinari, C.; Lupidi, G.; Scopelliti, R.; Mukhopadhyay, S.; Riedel, T.; Dyson, P. J. Ruthenium(II)−Arene RAPTA Type Complexes Containing Curcumin and Bisdemethoxycurcumin Display Potent and Selective Anticancer Activity. *Organometallics* **2014**, *33*, 3709−3715.

(24) Aman, F.; Hanif, M.; Kubanik, M.; Ashraf, A.; Söhnel, T.; Jamieson, S. M. F.; Siddiqui, W. A.; Hartinger, C. G. Anti-Inflammatory Oxicams as Multi-donor Ligand Systems: pH- and Solvent-Dependent Coordination Modes of Meloxicam and Piroxicam to Ru and Os. *Chem. - Eur. J.* **2017**, *23*, 4893−4902.

(25) Ang, W. H.; Parker, L. J.; De Luca, A.; Juillerat-Jeanneret, L.; Morton, C. J.; Lo Bello, M.; Parker, M. W.; Dyson, P. J. Rational Design of an Organometallic Glutathione Transferase Inhibitor. *Angew. Chem., Int. Ed.* **2009**, *48*, 3854−3857.

(26) Agonigi, G.; Riedel, T.; Zacchini, S.; Păunescu, E.; Pampaloni, G.; Bartalucci, N.; Dyson, P. J.; Marchetti, F. Synthesis and Antiproliferative Activity of New Ruthenium Complexes with Ethacrynic-Acid-Modified Pyridine and Triphenylphosphine Ligands. *Inorg. Chem.* **2015**, *54*, 6504−6512.

(27) Kurzwernhart, A.; Kandioller, W.; Bartel, C.; Bächler, S.; Trondl, R.; Mühlgassner, G.; Jakupec, M. A.; Arion, V. B.; Marko, D.; Keppler, B. K.; Hartinger, C. G. Targeting the DNA-topoisomerase complex in a double-strike approach with a topoisomerase inhibiting moiety and covalent DNA binder. *Chem. Commun.* **2012**, *48*, 4839−4841.

(28) Middleton, E.; Kandaswami, C.; Theoharides, T. C. The effects of plant flavonoids on mammalian cells: Implications for inflammation, heart disease, and cancer. *Pharmacol. Rev.* **2000**, *52*, 673−751.

(29) Cushnie, T. P. T.; Lamb, A. J. Antimicrobial activity of flavonoids. *Int. J. Antimicrob. Agents* **2005**, *26*, 343−356.

(30) Roshal, A. D.; Grigorovich, A. V.; Doroshenko, A. O.; Pivovarenko, V. G.; Demchenko, A. P. Flavonols as metal-ion

DOI: 10.1021/acs.inorgchem.8b01187
Inorg. Chem. XXXX, XXX, XXX−XXX

chelators: complex formation with Mg^{2+} and Ba^{2+} cations in the excited state. *J. Photochem. Photobiol., A* **1999**, *127*, 89−100.
(31) Sutter, M.; Oliveira, S.; Sanders, N. N.; Lucas, B.; van Hoek, A.; Hink, M. A.; Visser, A. J. W. G.; De Smedt, S. C.; Hennink, W. E.; Jiskoot, W. Sensitive spectroscopic detection of large and denatured protein aggregates in solution by use of the fluorescent dye Nile red. *J. Fluoresc.* **2007**, *17*, 181−192.
(32) Mladenka, P.; Macakova, K.; Filipsky, T.; Zatloukalova, L.; Jahodar, L.; Bovicelli, P.; Silvestri, I. P.; Hrdina, R.; Saso, L. In vitro analysis of iron chelating activity of flavonoids. *J. Inorg. Biochem.* **2011**, *105*, 693−701.
(33) Kubanik, M.; Tu, J. K. Y.; Söhnel, T.; Hejl, M.; Jakupec, M. A.; Kandioller, W.; Keppler, B. K.; Hartinger, C. G. Expanding on the Structural Diversity of Flavone-Derived Ruthenium^{II}(η^6-arene) Anticancer Agents. *Metallodrugs* **2015**, *1*, 24−35.
(34) el Amrani, F. B.-A.; Perelló, L.; Borrás, J.; Torres, L. Development of Novel DNA Cleavage Systems Based on Copper Complexes. Synthesis and Characterisation of Cu(II) Complexes of Hydroxyflavones. *Met. Based Drugs* **2000**, *7*, 365−370.
(35) Santos, J. P.; Zaniquelli, M. E. D.; De Giovani, W. F.; Galembeck, S. E. Aluminum ion complex formation with 3-hydroxyflavone in Langmuir and Langmuir−Blodgett films. *Colloids Surf., A* **2002**, *198−200*, 569−576.
(36) Dangleterre, L.; Cornard, J.-P. Interaction of lead(II) chloride with hydroxyflavones in methanol: A spectroscopic study. *Polyhedron* **2005**, *24*, 1593−1598.
(37) Lapouge, C.; Dangleterre, L.; Cornard, J.-P. Spectroscopic and Theoretical Studies of the Zn(II) Chelation with Hydroxyflavones. *J. Phys. Chem. A* **2006**, *110*, 12494−12500.
(38) Sathish, S.; Narayan, G.; Rao, N.; Janardhana, C. A Self-Organized Ensemble of Fluorescent 3-Hydroxyflavone-Al(III) Complex as Sensor for Fluoride and Acetate Ions. *J. Fluoresc.* **2006**, *17*, 1−5.
(39) Prajapati, R.; Dubey, S. K.; Gaur, R.; Koiri, R. K.; Maurya, B. K.; Trigun, S. K.; Mishra, L. Structural characterization and cytotoxicity studies of ruthenium(II)−dmso−chloro complexes of chalcone and flavone derivatives. *Polyhedron* **2010**, *29*, 1055−1061.
(40) Kurzwernhart, A.; Kandioller, W.; Bachler, S.; Bartel, C.; Martic, S.; Buczkowska, M.; Muhlgassner, G.; Jakupec, M. A.; Kraatz, H. B.; Bednarski, P. J.; Arion, V. B.; Marko, D.; Keppler, B. K.; Hartinger, C. G. Structure-Activity Relationships of Targeted Ru^{II}(η^6-p-Cymene) Anticancer Complexes with Flavonol-Derived Ligands. *J. Med. Chem.* **2012**, *55*, 10512−10522.
(41) Kurzwernhart, A.; Kandioller, W.; Enyedy, E. A.; Novak, M.; Jakupec, M. A.; Keppler, B. K.; Hartinger, C. G. 3-Hydroxyflavones vs. 3-hydroxyquinolinones: structure-activity relationships and stability studies on Ru^{II}(arene) anticancer complexes with biologically active ligands. *Dalton Trans.* **2013**, *42*, 6193−6202.
(42) Kurzwernhart, A.; Mokesch, S.; Klapproth, E.; Adib-Ravazi, M. S.; Jakupec, M. A.; Hartinger, C. G.; Kandioller, W.; Keppler, B. K. Flavonoid-Based Organometallics with Different Metal Centers − Investigations of the Effects on Reactivity and Cytotoxicity. *Eur. J. Inorg. Chem.* **2016**, *2016*, 240−246.
(43) Movassaghi, S.; Hanif, M.; Holtkamp, H. U.; Söhnel, T.; Jamieson, S. M. F.; Hartinger, C. G. Making organoruthenium complexes of 8-hydroxyquinolines more hydrophilic: impact of a novel l-phenylalanine-derived arene ligand on the biological activity. *Dalton Trans.* **2018**, *47*, 2192−2201.
(44) Fishman, W. H.; Green, S.; Inglis, N. I. L-phenylalanine: an organ specific, stereospecific inhibitor of human intestinal alkaline phosphatase. *Nature* **1963**, *198*, 685−686.
(45) Williams, D. B. G.; Lawton, M. Drying of Organic Solvents: Quantitative Evaluation of the Efficiency of Several Desiccants. *J. Org. Chem.* **2010**, *75*, 8351−8354.
(46) Dolomanov, O. V.; Bourhis, L. J.; Gildea, R. J.; Howard, J. A.; Puschmann, H. OLEX2: a complete structure solution, refinement and analysis program. *J. Appl. Crystallogr.* **2009**, *42*, 339−341.
(47) Sheldrick, G. Crystal structure refinement with SHELXL. *Acta Crystallogr., Sect. C: Struct. Chem.* **2015**, *71*, 3−8.
(48) Holtkamp, H. U.; Movassaghi, S.; Morrow, S. J.; Kubanik, M.; Hartinger, C. G. Metallomic study on the metabolism of RAPTA-C and cisplatin in cell culture medium and its impact on cell accumulation. *Metallomics* **2018**, *10*, 455−462.
(49) Chen, H.; Parkinson, J. A.; Morris, R. E.; Sadler, P. J. Highly Selective Binding of Organometallic Ruthenium Ethylenediamine Complexes to Nucleic Acids: Novel Recognition Mechanisms. *J. Am. Chem. Soc.* **2003**, *125*, 173−186.
(50) Olive, P. L.; Banáth, J. P. Kinetics of H2AX phosphorylation after exposure to cisplatin. *Cytometry, Part B* **2009**, *76B*, 79−90.

DOI: 10.1021/acs.inorgchem.8b01187
Inorg. Chem. XXXX, XXX, XXX−XXX